

Effect and Compensation of Symbol Timing Offset in OFDM Systems With Channel Interpolation

Dah-Chung Chang, *Member, IEEE*

Abstract—Symbol timing offset (STO) can result in intersymbol interference (ISI) and a rotated phase which value is proportional to the subcarrier index at the FFT output in an OFDM receiver. In order to avoid ISI, the FFT window start position has to be put in advance of the estimated point obtained by coarse STO estimation algorithms. But a large number of forward-shift samples will deteriorate the estimation of data subcarrier channels requiring interpolation from pilot subcarrier channels due to the phase rotation caused by a residual STO. In this paper we analyze the influence of STO on channel interpolation and propose a new compensation method for channel correction with STO. From the performance analysis of simulation results in the DVB-T application, the new algorithm not only has a better performance but also is attractive in using a simple residual STO estimation method such that few pilots are required for fine STO estimation compared to conventional approaches.

Index Terms—Channel interpolation, DVB-T, intersymbol interference, OFDM, symbol timing offset.

I. INTRODUCTION

ORTHOGONAL frequency division multiplexing (OFDM) takes advantage of low complexity and mature DSP technology to implement a multicarrier communication system by using IFFT/FFT, and it has been found in broad applications, e.g., WLAN IEEE 802.11a/n, Digital Audio Broadcasting (DAB), Digital Terrestrial Video Broadcasting (DVB-T) [1], IEEE 802.16a/e, Ultra-wideband (UWB). The OFDM receiver discriminates each of aliasing subcarriers through the FFT operation based on exact frequency positions of all received subcarriers. Hence, a stringent challenge for an OFDM system compared to a single-carrier communication system is that the OFDM system is more sensitive to synchronization imperfections, especially the influence of carrier frequency offset (CFO) [2], [3] and timing offset [4].

The timing offset problem involves symbol timing offset (STO) and sample timing offset. The former is a special issue in OFDM systems, and the latter is the same as that is met in single-carrier communication systems, known as sampling clock recovery. The OFDM receiver needs to know the appropriate FFT window position for the incoming sample stream,

Manuscript received June 17, 2007; revised June 30, 2008. First published October 03, 2008; current version published December 04, 2008. This work was supported in part by National Science Council of Taiwan under the contract 95-220-E-008-003.

The author is with the Department of Communication Engineering, National Central University, Jhongli, Taoyuan 320, Taiwan, R.O.C. (e-mail: dcchang@ce.ncu.edu.tw).

Color versions of one or more of the figures in this paper are available online at <http://ieeexplore.ieee.org>.

Digital Object Identifier 10.1109/TBC.2008.2002339

otherwise the interference named intersymbol interference (ISI) due to window overlapping between two successive OFDM symbols may be raised if the FFT window is put behind the real start position. In the DVB-T system, the channel is so complicated that STO needs to be carefully processed in order to keep the window start point within the ISI-free region of cyclic prefix (CP) for each symbol. The sample frequency offset results from the sampling clock mismatch between the transmitter and the receiver. It was shown in [5] that the sample timing offset can cause severe intercarrier interference (ICI) in an OFDM system with a large number of subcarriers

For the OFDM systems with a preamble, STO can be estimated by calculating the position of maximum correlation of the received signal and the preamble sequence [6]. For the system without a preamble, the maximum likelihood estimation (MLE) algorithm [7] is an effective technique to coarsely determine STO by exploring the peak value of the correlation between the input signal and its delayed version. In [8], the synchronization parameters are also found by applying the MLE method to a pre-defined pseudo-noise sequence which is added to both the OFDM symbol and the CP in the time domain. However, the MLE algorithm has high estimation fluctuation for a long channel impulse response (CIR) delay spread and at low SNR. Some designs [9], [10], [17] solved the STO problem by first adding a pre-advance offset to the coarsely estimated FFT position to avoid ISI, where the residual STO causes a rotated phase which value is proportional to the subcarrier index. If the OFDM system has regular pilots inserted on all subcarriers, the FFT output signals and the estimated channel responses will simultaneously carry the same rotated phase which can be eliminated by channel equalization in obtaining the estimates of transmitted signals. Hence the fine symbol timing control is not essential when the sample timing correction can be performed independently. But in some systems, like DVB-T, the estimated channel responses of data subcarriers are obtained by interpolating the channel responses of scattered pilot subcarriers such that the accuracy of channel estimation could be seriously degraded due to the interpolation with differently rotated phases at pilot subcarriers. Hence, de-rotated FFT output signals are required [11]–[13] for channel interpolation with a residual STO. In order to obtain more accurate symbol timing control, some fine STO estimation methods have been proposed [14]–[22] to estimate the residual timing offset after the coarse STO correction. One approach is to estimate the CIR time delay by the IFFT operation with zero padding at pilot subcarriers [17]–[19]. Another main approach calculates the rotated phase on all pilot subcarriers at the FFT output to obtain accurate estimation [14]–[16], [20], [22]. However, these two approaches require intensive computations for fine STO estimation in order

to avoid ISI. More research works review on the synchronization scheme for either continuous transmission mode or burst packet transmission mode can be found in [22].

In this paper, we analyze the effect of STO on channel estimation in a pilot-aided OFDM system and propose a new compensation method for channel correction with a residual STO. Although the application to 2K mode DVB-T system is illustrated as an example here, the proposed method can be applied to mobile OFDM systems with similar pilot pattern. For the implementation consideration, the linear channel interpolation is usually used in the frequency direction [23]–[25], which is also assumed in our analysis. In the new method, the compensation factor is not sensitive to STO estimation accuracy such that no ISI problem will be raised. Hence a simple residual STO estimation method for DVB-T is proposed as well in order to reduce the computational requirement.

II. SYSTEM MODEL AND ESTIMATION OF SYMBOL TIMING OFFSET

Assume that $X_{l,k}$ is the transmitted baseband signal at the k th subcarrier of the l th symbol in an ideal N -subcarrier OFDM system. The FFT output data at the k th subcarrier, $Y_{l,k}$, can be written as

$$Y_{l,k} = H_{l,k}X_{l,k} + W_{l,k}, \quad l \geq 0, \quad 0 \leq k \leq N-1 \quad (1)$$

where $H_{l,k}$ and $W_{l,k}$ represent the frequency responses of the channel and the additive white Gaussian noise (AWGN), respectively. Let $y_{l,n}$ be the received signal before FFT and θ the normalized STO with respect to the sample duration, where θ is a positive integer number within the ISI-free region. The FFT output signals due to the STO become

$$\begin{aligned} Y_{l,k}^\theta &= \sum_{n=0}^{N-1} y_{l,n-\theta} e^{-j2\pi kn/N} \\ &= e^{-j2\pi k\theta/N} \cdot Y_{l,k} \end{aligned} \quad (2)$$

Equation (2) indicates that STO within the ISI-free region causes phase rotation with respect to the ideal output at all subcarriers. If θ is negative, STO makes the FFT window contain some samples of the next symbol and thus, ISI is induced.

In a pilot-aided OFDM system, the channel estimation is obtained through pilots that are inserted between data tones. For simplicity, we divide the N subcarriers into *pilot subcarriers* containing pilots and *data subcarriers* containing only data as shown in Fig. 1. Assume that the pilot tone power is normalized, the estimated channel responses at pilot subcarriers can be obtained by the least squares (LS) method:

$$\begin{aligned} \hat{H}_{l_p,k}^\theta &= Y_{l_p,k}^\theta \cdot X_{l_p,k}^* \\ &= e^{-j2\pi k\theta/N} \hat{H}_{l_p,k} \end{aligned} \quad (3)$$

where $X_{l_p,k}$ is a pilot tone with l_p denoting its symbol index and $\hat{H}_{l_p,k} = H_{l_p,k} + W_{l_p,k}X_{l_p,k}^*$. By neglecting the noise term in (3), the estimated channel responses are also phase-rotated by θ with respect to their correct versions. In practical applications, the symbol duration is usually designed to be so small that the

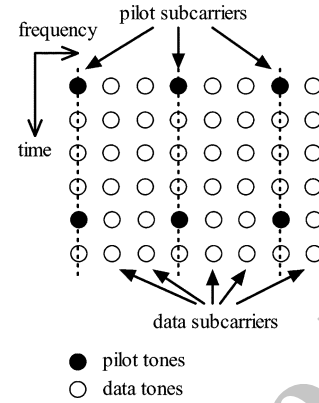


Fig. 1. Pilot subcarriers and data subcarriers in an OFDM signal.

channel responses between two pilots are almost time-invariant. Then, the channel responses of data tones at pilot subcarriers can apply the estimated channel responses of the latest pilots, i.e., $\hat{H}_{l_d,k}^\theta \approx \hat{H}_{l_p,k}^\theta$ where l_d denotes the symbol index of a data tone behind the latest pilot symbol index l_p , which also implies $\hat{H}_{l_d,k}^\theta \approx e^{-j2\pi k\theta/N} H_{l_d,k}$. By the LS method, data at pilot subcarriers can be directly recovered by

$$\begin{aligned} \hat{X}_{l_d,k}^\theta &= Y_{l_d,k}^\theta / \hat{H}_{l_d,k}^\theta \\ &\approx X_{l_d,k} + W_{l_d,k} / \hat{H}_{l_d,k} \end{aligned} \quad (4)$$

Equation (4) means that at pilot subcarriers, the equalized outputs of data tones are free from the effect of STO even though the phases of estimated channel responses are rotated due to STO.

For data subcarriers, channel responses are usually obtained by their neighboring pilot subcarriers. In consequence, the erroneous results are generated due to the interpolation of estimated channel responses with differently rotated phases [12], [14]. Hence, to correct STO in advance of channel interpolation is unavoidable for an OFDM system with data subcarriers. The MLE algorithm proposed in [7] is an effective method for “coarse STO estimation,” which uses the CP information and is independent of CFO and sample timing error. The purpose of coarse STO estimation is to initialize a positive θ value for the FFT window operation. The following recursive routines can be used to enhance the estimation of a coarse STO [17]:

$$\gamma_t(\theta) = \sum_{n=\theta}^{\theta+N_g-1} r_t(n)r_t^*(n+N) \quad (5)$$

$$\bar{\gamma}_t(\theta) = \alpha \bar{\gamma}_{t-1}(\theta) + (1-\alpha)\gamma_t(\theta) \quad (6)$$

$$\hat{\theta}_t = \arg \max_{\theta} \{|\bar{\gamma}_t(\theta)|\} \quad (7)$$

where $r_t(n)$ is the received signal at time t , N_g is the length of CP, $\hat{\theta}_t$ is the estimated STO, and α is a forgetting factor for smoothing noise. The estimated STO $\hat{\theta}_t$ is used to control the FFT window. However, the algorithm introduces an estimation error relying on the channel environment. To obtain a positive θ not to cause ISI, the shift of several samples (usually more than tens of samples for the DVB-T application in the multipath fading channel) in advance of the estimated position is required. Then the rotated phase at the FFT output can be

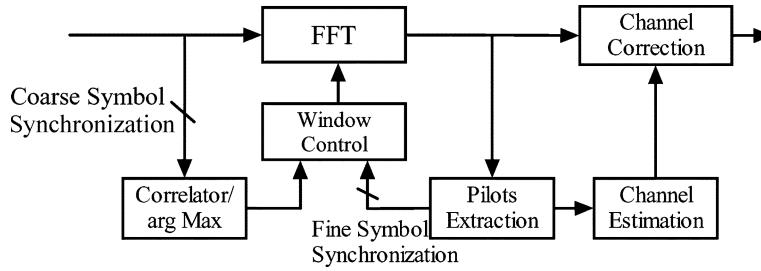


Fig. 2. Structure of conventional symbol timing synchronization.

calculated through the extracted pilots to find more accurate θ which is fed back to control the FFT window for eliminating the residual STO. This process is usually known as the “fine STO estimation.” The functional block of the conventional STO correction concept is depicted in Fig. 2.

III. THE NEW STO CORRECTION METHOD

In the fine STO estimation process, inaccurate estimation will result in residual STO which can cause ISI and incorrect channel interpolation at data subcarriers. The conventional methods for fine STO estimation usually need to calculate a lot of pilots with intensive computations. The concepts of two conventional approaches to estimating the fine STO value are depicted in Fig. 3. In Fig. 3(a), the STO is obtained by figuring out the slope of the phases of pilot subcarriers after the frequency domain equalization [15], which can be referred to (3) with removing the channel effect through estimated channel responses. Hence, in a severe frequency selective fading channel, accurate channel estimation and lots of pilots are required to improve the estimation accuracy of the fine STO. For example in the DVB-T system, hundreds of scattered pilots may be involved for the fine STO estimation by this method. The other method in Fig. 3(b) uses pilot subcarriers to estimate the CIR [17]. However, the CIR is obtained through the IFFT operation of the estimated frequency responses at pilot subcarriers and zero padding at data subcarriers. The high computational complexity of the IFFT operation is introduced in this method. Beside the issue of intensive computations, the above methods do not guarantee accurate estimation. In general cases, more than 10 samples of estimation offset can be observed [23]. That is, a forward-shift for the FFT window is also required for preventing ISI even though the number of forward-shift with fine STO estimation is less than that with coarse STO estimation [9].

The proposed STO correction technique allows a positive residual STO value for channel interpolation such that ISI is not caused. As the result delineated in (4), the equalized outputs at pilot subcarriers do not yield phase rotation with the positive residual STO. We explore the effect of channel interpolation at data subcarriers and compensate it by applying a simple STO estimation method with few pilots since the new method is not concerned with ISI. Hence, a few of pilots can be used for STO estimation with reduced computations compared to conventional methods. Moreover, the effect of forward-shift for the FFT window on channel interpolation is alleviated in the

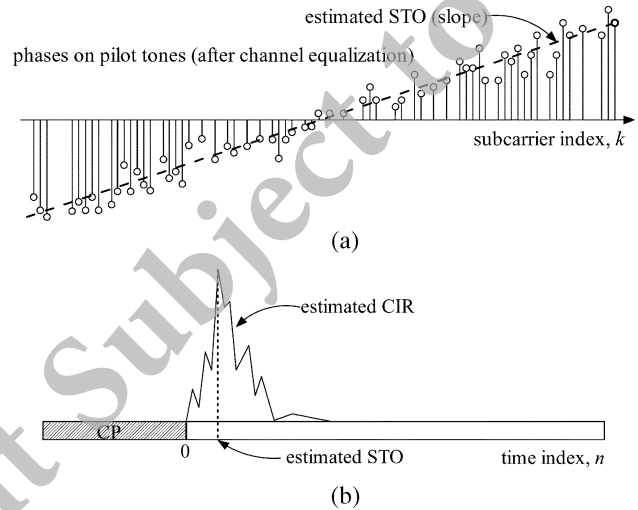


Fig. 3. The concepts of two conventional approaches to estimating the fine STO value: (a) phase rotation on pilot subcarriers due to STO; (b) CIR estimate due to STO.

new method. We use the 2K mode DVB-T system to explain the new method.

A. Channel Correction With STO and Linear Interpolation

In the DVB-T system, the scattered pilots used for channel estimation are spread in both time and frequency directions. As shown in Fig. 4, the DVB-T pilot pattern includes data subcarriers (marked as k and $k + 1$) and scattered pilot subcarriers (marked as $k - 1$ and $k + 2$) in addition to continual pilot subcarriers and transmission parameter signaling (TPS) carriers [1]. There is one scattered pilot out of four symbols in the time direction and one scattered pilot out of twelve subcarriers in the frequency direction. Data are transmitted at active subcarriers without pilot tones. The channel responses of pilot tones can be estimated directly by the LS method while the channel responses at data subcarriers are calculated by interpolation of the values obtained from pilot tones. If the channel is slow fading, the channel responses of data subcarriers are usually obtained by nearest neighbor or linear interpolation [11] of two neighboring pilots at the same subcarrier index where the data can be recovered without rotated phases as described in (4). Assuming the linear interpolation method is also used in the frequency direction, the output data between two neighboring pilot subcarriers with a residual STO can be calculated as follows.

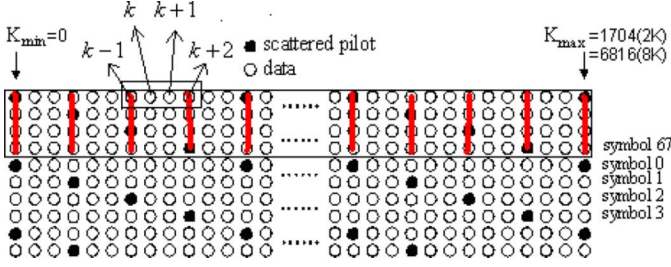


Fig. 4. DVB-T scattered pilots.

By (3), the channel response at subcarrier k can be obtained from the estimated channel responses at pilot subcarriers $k-1$ and $k+2$

$$\begin{aligned}\hat{H}_{l,k}^\theta &= \frac{2}{3}\hat{H}_{l,k-1}^\theta + \frac{1}{3}\hat{H}_{l,k+2}^\theta \\ &= e^{-j2\pi(k-1)\theta/N} \cdot \left[\hat{H}_{l,k} + \frac{1}{3}(e^{-j6\pi\theta/N} - 1) \cdot \hat{H}_{l,k+2} \right] \\ &= e^{-j2\pi(k-1)\theta/N} \cdot \hat{H}_{l,k}(1 + \hat{\varepsilon}_{l,k})\end{aligned}\quad (8)$$

where $\hat{\varepsilon}_{l,k}$ is given by

$$\begin{aligned}\hat{\varepsilon}_{l,k} &= \frac{1}{3}(e^{-j6\pi\theta/N} - 1) \cdot \frac{\hat{H}_{l,k+2}}{\hat{H}_{l,k}} \\ &= \varepsilon(\theta) \cdot \hat{\alpha}_{l,k}\end{aligned}\quad (9)$$

where $\varepsilon(\theta)$ and $\hat{\alpha}_{l,k}$ denote $(e^{-j6\pi\theta/N} - 1)/3$ and $\hat{H}_{l,k+2}/\hat{H}_{l,k}$, respectively. By (2) and (8), the equalized output is

$$\begin{aligned}\hat{X}_{l,k}^\theta &= \frac{Y_{l,k}^\theta}{\hat{H}_{l,k}^\theta} \\ &= \frac{e^{-j2\pi\theta/N}}{1 + \hat{\varepsilon}_{l,k}} \cdot \hat{X}_{l,k}\end{aligned}\quad (10)$$

By (10), the correct transmitted data $\hat{X}_{l,k}$ can be obtained from $\hat{X}_{l,k}^\theta$ as

$$\hat{X}_{l,k} = e^{j2\pi\theta/N}(1 + \hat{\varepsilon}_{l,k}) \cdot \hat{X}_{l,k}^\theta.\quad (11)$$

Similarly, the interpolated channel response at subcarrier $k+1$ is

$$\begin{aligned}\hat{H}_{l,k+1}^\theta &= \frac{2}{3}\hat{H}_{l,k+2}^\theta + \frac{1}{3}\hat{H}_{l,k-1}^\theta \\ &= e^{-j2\pi(k+2)\theta/N} \cdot \hat{H}_{l,k+1}(1 + \hat{\varepsilon}_{l,k+1})\end{aligned}\quad (12)$$

where $\hat{\varepsilon}_{l,k+1}$ is given by

$$\begin{aligned}\hat{\varepsilon}_{l,k+1} &= \frac{1}{3}(e^{j6\pi\theta/N} - 1) \cdot \frac{\hat{H}_{l,k-1}}{\hat{H}_{l,k+1}} \\ &= \varepsilon(-\theta) \cdot \hat{\alpha}_{l,k+1}\end{aligned}\quad (13)$$

where $\hat{\alpha}_{l,k+1}$ denotes $\hat{H}_{l,k-1}/\hat{H}_{l,k+1}$. The equalized output is

$$\begin{aligned}\hat{X}_{l,k+1}^\theta &= \frac{Y_{l,k+1}^\theta}{\hat{H}_{l,k+1}^\theta} \\ &= \frac{e^{j2\pi\theta/N}}{1 + \hat{\varepsilon}_{l,k+1}} \cdot \hat{X}_{l,k+1}\end{aligned}\quad (14)$$

By (14), the correct transmitted data $\hat{X}_{l,k+1}$ can be obtained from $\hat{X}_{l,k+1}^\theta$ as

$$\hat{X}_{l,k+1} = e^{-j2\pi\theta/N}(1 + \hat{\varepsilon}_{l,k+1}) \cdot \hat{X}_{l,k+1}^\theta.\quad (15)$$

In (11) and (15), the calculation of $\hat{X}_{l,k}$ and $\hat{X}_{l,k+1}$ requires $\hat{\varepsilon}_{l,k}$ and $\hat{\varepsilon}_{l,k+1}$ and hence from (9) and (13), $\hat{\alpha}_{l,k}$ and $\hat{\alpha}_{l,k+1}$ have to be obtained in advance. From the definition of $\alpha_{l,k}$ and $\alpha_{l,k+1}$, the following recursive equations can be used to estimate parameters $\alpha_{l,k}$ and $\alpha_{l,k+1}$:

$$\hat{\alpha}_{l,k} = (1 - \beta)\hat{\alpha}_{l-1,k} + \beta \frac{\hat{H}_{l,k+2}}{\hat{H}_{l,k}},\quad (16)$$

and

$$\hat{\alpha}_{l,k+1} = (1 - \beta)\hat{\alpha}_{l-1,k+1} + \beta \frac{\hat{H}_{l,k-1}}{\hat{H}_{l,k+1}}\quad (17)$$

where β is a forgetting factor which controls the convergence rate and the steady-state mean squared error and $0 < \beta \leq 1$. However, the non-rotated channel responses $\hat{H}_{l,k}$ and $\hat{H}_{l,k+1}$ cannot be applied until we have obtained the results of $\hat{\varepsilon}_{l,k}$ and $\hat{\varepsilon}_{l,k+1}$ from (8) and (12). As we assume that the channel does not change significantly between two successive symbols, $\hat{H}_{l,k+2}/\hat{H}_{l,k} \approx \hat{H}_{l-1,k+2}/\hat{H}_{l-1,k}$ and $\hat{H}_{l,k-1}/\hat{H}_{l,k+1} \approx \hat{H}_{l-1,k-1}/\hat{H}_{l-1,k+1}$. By using (8) and (12), $\alpha_{l,k}$ and $\alpha_{l,k+1}$ in (16) and (17) can be estimated from the phase-rotated channel responses:

$$\hat{\alpha}_{l,k} = (1 - \beta)\hat{\alpha}_{l-1,k} + \beta \cdot e^{j6\pi\theta/N}(1 + \hat{\varepsilon}_{l-1,k}) \cdot \frac{\hat{H}_{l-1,k+2}}{\hat{H}_{l-1,k}},\quad (18)$$

and

$$\begin{aligned}\hat{\alpha}_{l,k+1} &= (1 - \beta)\hat{\alpha}_{l-1,k+1} + \beta \cdot e^{-j6\pi\theta/N} \\ &\quad \times (1 + \hat{\varepsilon}_{l-1,k+1}) \cdot \frac{\hat{H}_{l-1,k-1}}{\hat{H}_{l-1,k+1}}.\end{aligned}\quad (19)$$

The recursive computation of (18) and (19) requires initial values $\hat{\alpha}_{0,k}$ and $\hat{\alpha}_{0,k+1}$. Since most of the neighboring subcarriers have similar channel responses, we can set the initials as unity.

To explore the effect of STO on channel correction, we consider the special case when the channel is AWGN, i.e. $\alpha_{l,k+1} = \alpha_{l,k} = 1$. By (10) and (14), the equalized output suffers from

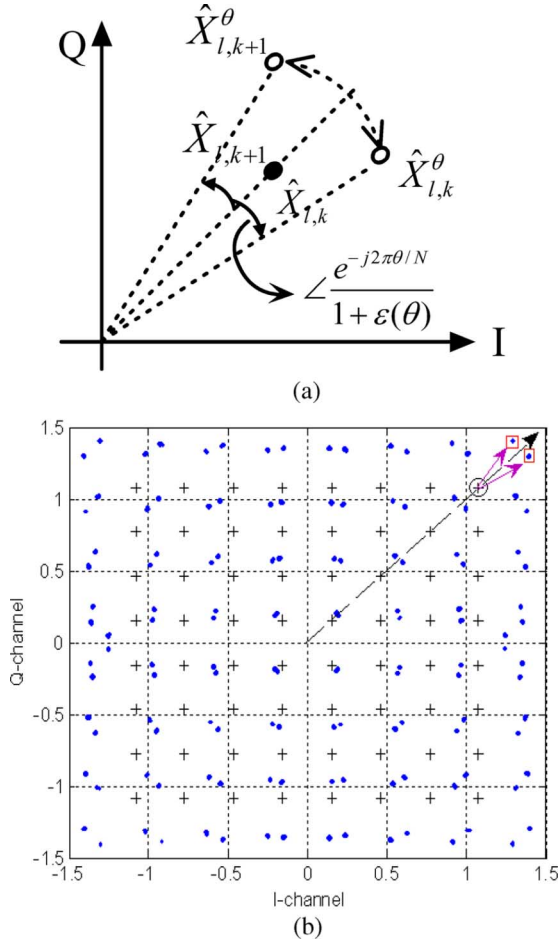


Fig. 5. The STO effect on the linearly interpolated data subcarriers: (a) conceptual illustration; (b) simulated results of the 64-QAM DVB-T signal constellation with STO = 150 and AWGN of SNR = 50 dB. The ideal position is at (1.08, 1.08). The new lower position is at (1.402, 1.298), and the new upper position is at (1.298, 1.402).

a constant rotated phase either in the negative or positive direction according to the subcarrier index being k or $k + 1$ due to a positive STO:

$$\angle \frac{e^{-j2\pi\theta/N}}{1+\varepsilon(\theta)} = -\angle \frac{e^{j2\pi\theta/N}}{1+\varepsilon(-\theta)}. \quad (20)$$

Besides, the amplitude is similarly amplified:

$$\left| \frac{e^{-j2\pi\theta/N}}{1+\varepsilon(\theta)} \right| = \left| \frac{e^{j2\pi\theta/N}}{1+\varepsilon(-\theta)} \right| \geq 1 \quad (21)$$

where the equality holds when $\theta = 0$.

The effect of STO on linearly interpolated data subcarriers is illustrated in Fig. 5(a) and 5(b), where we show the 64-QAM signal constellation after the channel equalization for 150 samples of STO with AWGN of SNR 50 dB. From Fig. 5(b) we can see that two new constellation positions in place of the ideal constellation position are observed due to STO. The new positions are consistent with the analytic results obtained by calculating the coordinate references. The farther the received signal from the origin of the constellation, the larger is the symbol error probability of the signal.

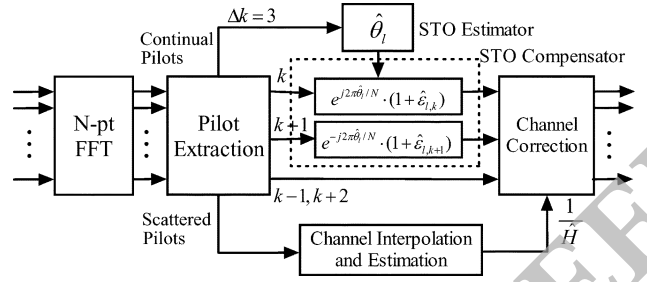


Fig. 6. Functional block of the proposed STO compensation technique.

B. Estimation of the Residual STO

The residual CFO and STO within the ISI-free region can result in phase offset at the FFT output. Let δ_f denote the normalized residual CFO. Consider k_{C1} and k_{C2} as the subcarrier indices of two continual pilots. The received signals at these two subcarriers are [11]

$$Y_{l,k_{Ci}}^\theta = e^{-j2\pi(k_{Ci}\theta/N - l\delta_f + \phi_0)} H_{l,k_{Ci}} X_{l,k_{Ci}} + W_{l,k_{Ci}}, \quad i = 1, 2 \quad (22)$$

where ϕ_0 is a constant phase offset. Let $S_{\Delta k}$ be the set containing the elements of two continual pilots with index difference Δk , that is, $S_{\Delta k} = \{(k_{C1}, k_{C2}) | \Delta k = k_{C2} - k_{C1}\}$. In order to obtain the value of θ , we choose Δk as small as possible so that

$$H_{l,k_{C1}} \cdot H_{l,k_{C2}}^* \approx |H_{l,k_{C1}}|^2. \quad (23)$$

For the 2K mode DVB-T system, $\Delta k = 3$ is the minimal value with all of the elements being on $(k_{C1}, k_{C2}) = (279, 282), (939, 942), (1107, 1110),$ and $(1137, 1140)$. By using (23) and assuming the power of the continual pilot is normalized, we can have the following calculation:

$$\begin{aligned} & \sum_{k \in S_{\Delta k}} (Y_{l,k_{C1}}^\theta \cdot X_{l,k_{C1}}^*) (Y_{l,k_{C2}}^\theta \cdot X_{l,k_{C2}}^*)^* \\ & \approx \sum_{k \in S_{\Delta k}} \left[e^{j2\pi\Delta k \cdot \theta/N} \cdot |H_{l,k_{C1}}|^2 + W_l'(k_{C1}, k_{C2}) \right] \\ & = e^{j2\pi\Delta k \cdot \theta/N} \cdot \sum_{k \in S_{\Delta k}} [|H_{l,k_{C1}}|^2 + W_l(k_{C1}, k_{C2})] \end{aligned} \quad (24)$$

where $W_l'(k_{C1}, k_{C2})$ and $W_l(k_{C1}, k_{C2})$ are noisy terms. From (24), the residual STO value can be estimated by

$$\hat{\theta}_l = \frac{N}{2\pi \cdot \Delta k} \cdot \angle \sum_{k \in S_{\Delta k}} (Y_{l,k_{C1}}^\theta X_{l,k_{C1}}^*) \cdot (Y_{l,k_{C2}}^\theta X_{l,k_{C2}}^*)^*. \quad (25)$$

The estimation range is

$$0 \leq \hat{\theta}_l \leq \frac{N}{2 \cdot \Delta k}. \quad (26)$$

In this case, the maximum STO value able to be estimated is 341. Note that the pilot sets with larger Δk can be considered in (25), but the estimation range will be smaller for larger Δk and the accuracy of the approximation in (23) may be a concern. When a large value of Δk is used, the channel effect can

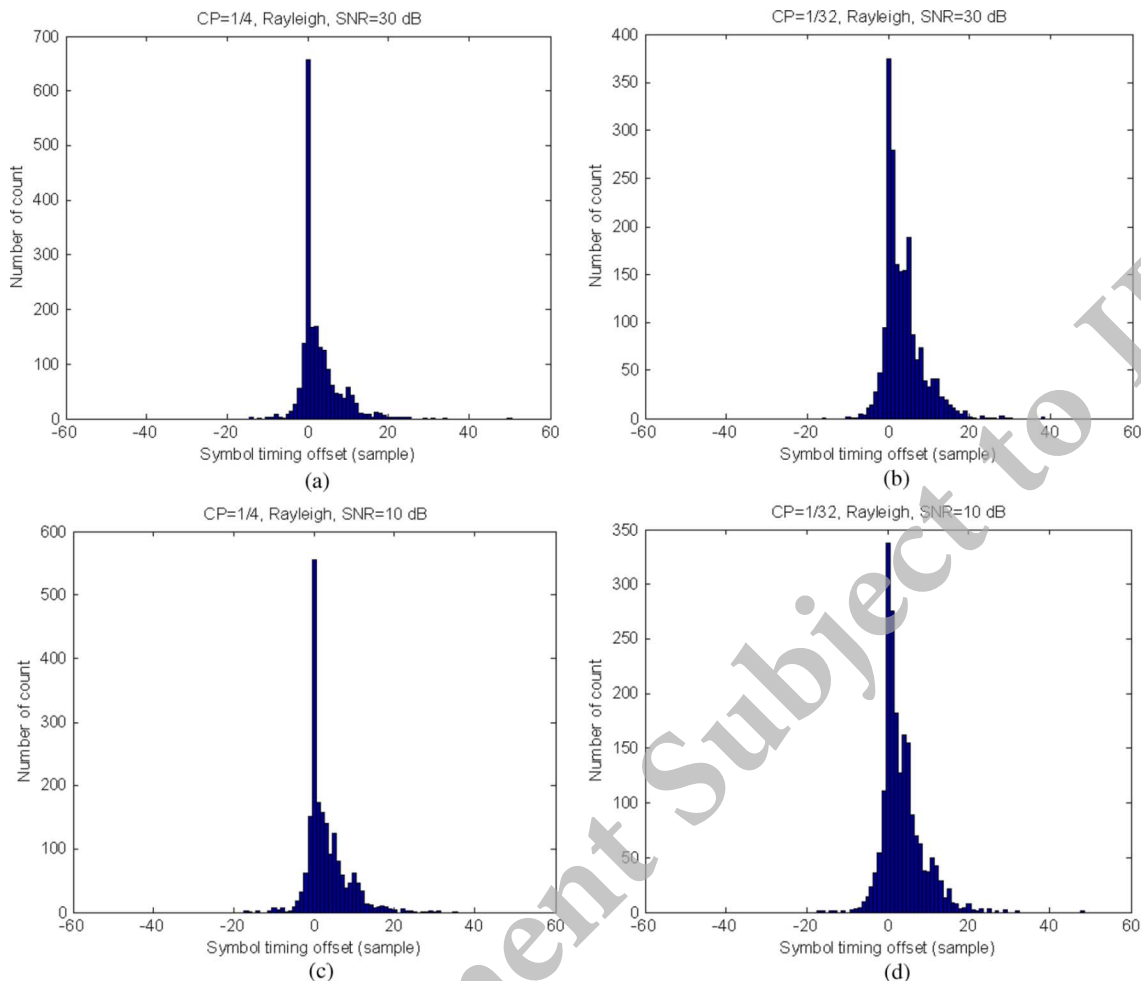


Fig. 7. The histograms of the estimated coarse STO value in the Rayleigh fading channel. (a) CP = 1/4 and SNR = 30 dB. (b) CP = 1/32 and SNR = 30 dB. (c) CP = 1/4 and SNR = 10 dB. (d) CP = 1/32 and SNR = 10 dB.

be better removed in advance by using the estimated channel responses. In our simulations, the set for $\Delta k = 3$ is shown to have a satisfactory performance.

The estimated STO value obtained by (25) is then applied to (9), (11), (13), (15), (18), and (19) to constitute the proposed STO compensation technique which is depicted in Fig. 6.

IV. SIMULATION RESULTS

We consider the 64-QAM wireless transmission in the 2K mode DVB-T system with the guard interval of 1/4 symbol duration. The multipath channel models have a 20-tap delay spread based on a slight modification of the Rayleigh fading channel and the Rician channel as described in Annex B in the DVB-T standard [1]. However, the original channel proposal in [1] is described in the continuous-time domain, we use the discrete-time version for our simulations according to the sampling rate of the 8MHz bandwidth specification. The carrier frequency offset is set to be 32.4 (an arbitrary number) subcarriers of frequency spacing. In the beginning, we use the MLE algorithm to estimate coarse STO and coarse fractional CFO in the acquisition mode, and then the integer CFO and residual CFO tracking loop are used for CFO correction [26]. A scattered pilot mode determination scheme is also developed to distinguish data subcarriers,

scattered pilot subcarriers, continual pilot subcarriers, and TPS carriers [10], [27].

Fig. 7 show the histograms of the estimated coarse STO value in the multipath fading channel with SNR = 30 dB and 10 dB. By counting the numbers of zero symbol timing offset in the four cases, we can see that the estimation accuracy is obviously affected by the length of CP. Taking into consideration the fading channel effect, the appropriate forward-shift number for the FFT window to avoid ISI is usually more than tens of samples due to the MLE estimation error. Hence, 100 samples of forward-shift are chosen to control the FFT start point for coarse STO correction in our simulations.

Fig. 8 plots the constellation diagram of received signals with CFO = 32.4, the residual STO of 100 samples, and infinite SNR. The result shows that the constellation is perfectly rotated without ISI due to the effect of a positive STO and this also verifies the pilot extraction and CFO correction algorithms in our simulation model.

To show the efficiency of the proposed algorithm, we compare the un-compensated constellation and the compensated constellation after channel equalization with 30 dB SNR. Fig. 9(a)–(d) are the constellation diagrams of received signals with 100 samples of forward-shift to the coarse STO estimate

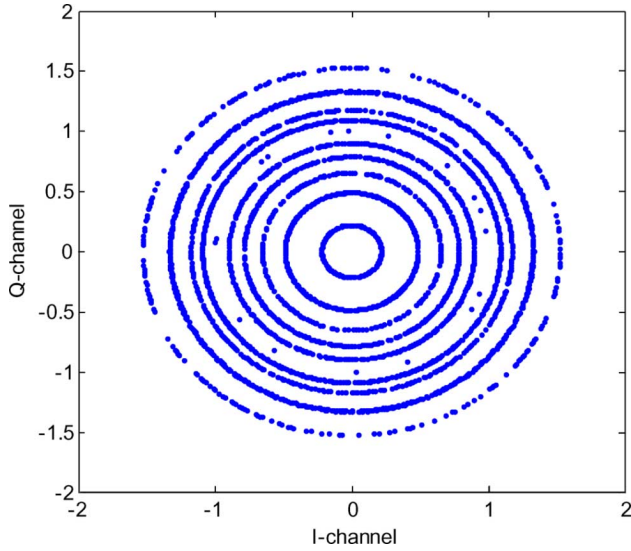


Fig. 8. The received signal constellation before channel correction with CFO = 32.4, STO = 100, and infinite SNR.

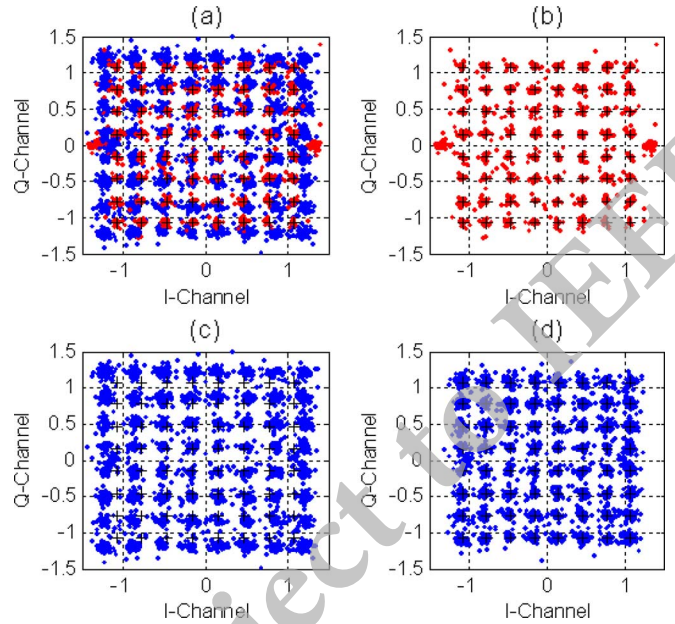


Fig. 10. Received signal constellation diagrams after channel correction with CFO = 32.4 and STO = 100 in the multipath Rayleigh fading channel and SNR = 30 dB: (a) mixture of data and pilots; (b) data at scattered pilot subcarrier indices; (c) data at the subcarrier indices without pilots; (d) corrected constellation of (c) by the proposed algorithm.

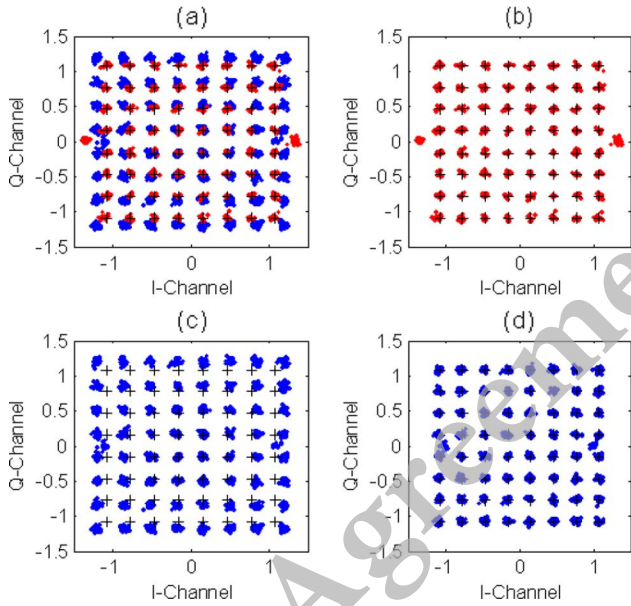


Fig. 9. Received signal constellation diagrams after channel correction with CFO = 32.4 and STO = 100 in the AWGN channel and SNR = 30 dB: (a) mixture of data and pilots; (b) data at scattered pilot subcarrier indices; (c) data at the subcarrier indices without pilots; (d) corrected constellation of (c) by the proposed algorithm.

in the AWGN channel. The leading FFT start position makes received signals violate the ideal constellation such that the symbol error rate rises. This is apparent from Fig. 9(a) which includes data and pilot tones, the constellation is significantly disturbed. In Fig. 9(b) and (c), we separate equalized outputs according to the subcarrier index containing scattered pilots (i.e. index numbers $k - 1$ and $k + 2$ as indicated in Fig. 4) and the subcarrier index not containing pilots (i.e. index numbers k and $k + 1$), respectively. In Fig. 9(b), data at those indices containing pilots are not calculated by the interpolated channel responses of neighboring subcarriers, the effect of STO due to interpolation is not present and the rotated phases can be

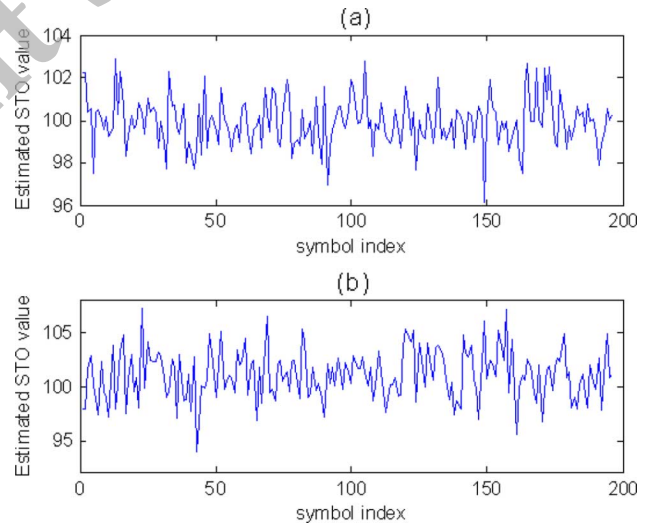


Fig. 11. The estimated STO value with CFO = 32.4, STO = 100, and SNR = 30 dB: (a) AWGN channel model; (b) the multipath Rayleigh fading channel model.

essentially corrected by the channel equalization in light of (4). In Fig. 9(c), STO distorts the interpolated data at subcarriers without pilots. Based on the proposed technique, the corrected constellation of Fig. 9(c) is shown in Fig. 9(d). The case in the multipath Rayleigh fading channel has similar results as the case in the AWGN channel as shown in Fig. 10(a)–(d).

The estimated STO values by (25) in the AWGN and the multipath Rayleigh fading channels are shown in Fig. 11(a) and (b), respectively. The estimation variation for the Rayleigh channel is larger than that for the AWGN channel at the same SNR level. Higher SNR level can achieve lower variation with almost one

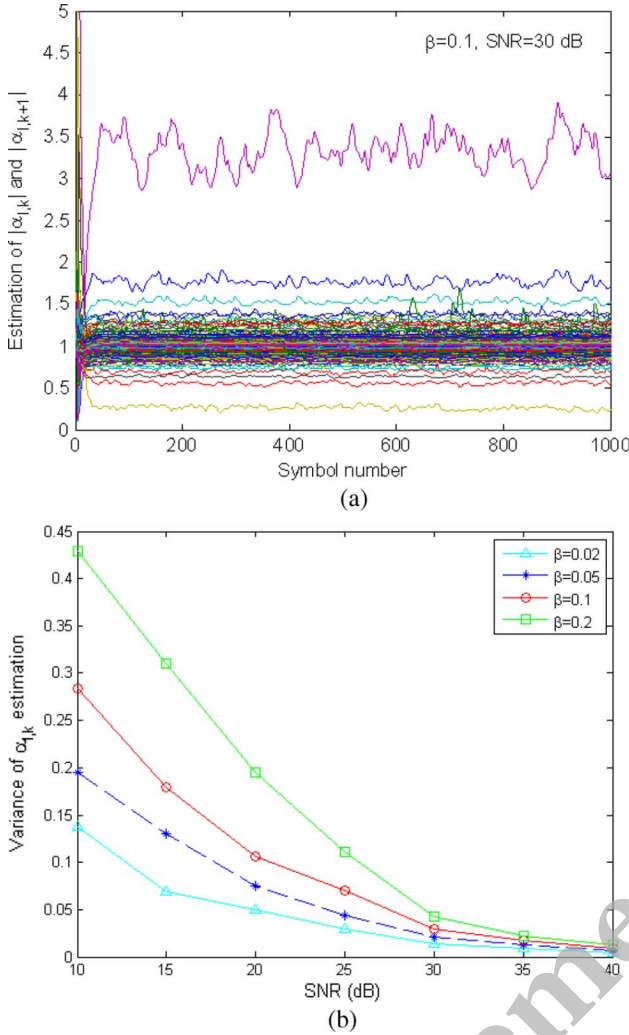


Fig. 12. (a) The tracking curves of the estimation of $|\alpha_{l,k}|$ and $|\alpha_{l,k+1}|$ in the multipath Rayleigh fading channel with 30 dB SNR; (b) variance of $\alpha_{l,k}$ estimation for different β and SNR values.

sample. In our simulation, there are maximum about ten samples of estimation error for the multipath fading channel. Although we can incorporate more pilots for STO estimation, the proposed compensation method resists to this estimation variation with an enough performance.

The tracking curves of the estimation of $|\alpha_{l,k}|$ and $|\alpha_{l,k+1}|$ in the multipath Rayleigh fading channel with 30 dB SNR are shown in Fig. 12(a). From the figure, we can see that most of the values are near unity. This can be explained as that channel responses for neighboring subcarriers are similar. However, there are some values larger than or less than unity, especially at the subcarriers with deep fading. In this simulation, we simply set the parameter β in (16) and (17) as 0.1. At low SNR, smaller β values can be chosen to reduce the variation of the estimation of $|\alpha_{l,k}|$ and $|\alpha_{l,k+1}|$. The variance of the estimation of $\alpha_{l,k}$ for different β and SNR values in the multipath Rayleigh fading channel are compared in Fig. 12(b). We can see that the estimation variance decreases as β decreases and increases as SNR decreases because that the accuracy of channel estimation is restricted by deeply fading subcarriers at low SNR.

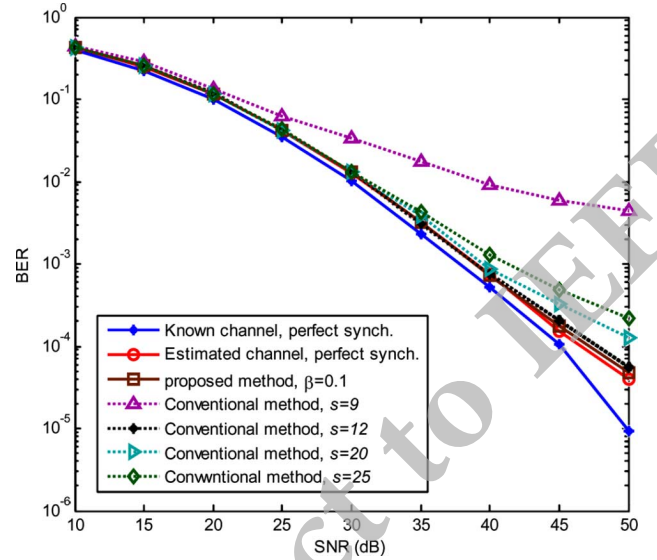


Fig. 13. Comparison of BER curves in the multipath Rayleigh fading channel for the known channel and perfect synchronization case, the proposed STO compensation method, and the conventional approach with different forward-shift samples.

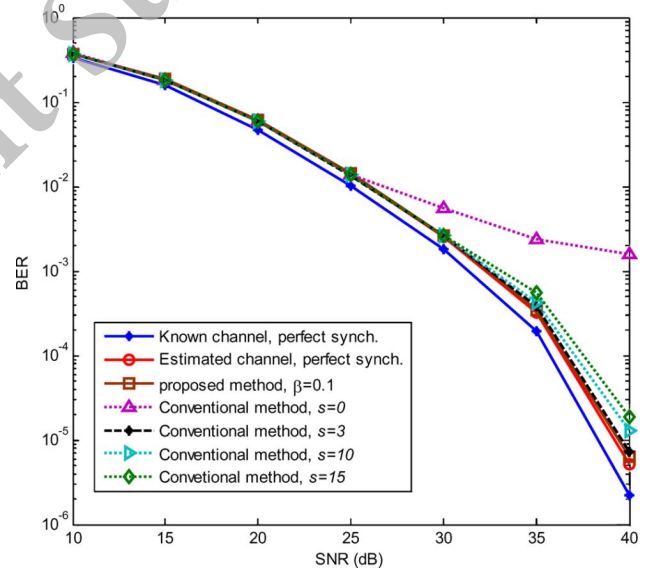


Fig. 14. Comparison of BER curves in the multipath Rician channel for the known channel and perfect synchronization case, the proposed STO compensation method, and the conventional approach with different forward-shift samples.

The BER performance comparison in the Rayleigh fading channel and the Rician channel are shown in Figs. 13 and 14, respectively. The curve of the best performance is assumed to have known channel responses and perfect synchronization. The estimated channel responses are obtained by LS estimation and linear interpolation in both time and frequency directions. Although the LS estimation and linear interpolation method does render little performance loss at high SNR, it is very attractive in implementation. For the purpose of comparison, the conventional STO correction method uses the proposed residual STO estimation method (25) as well. However, the proposed method

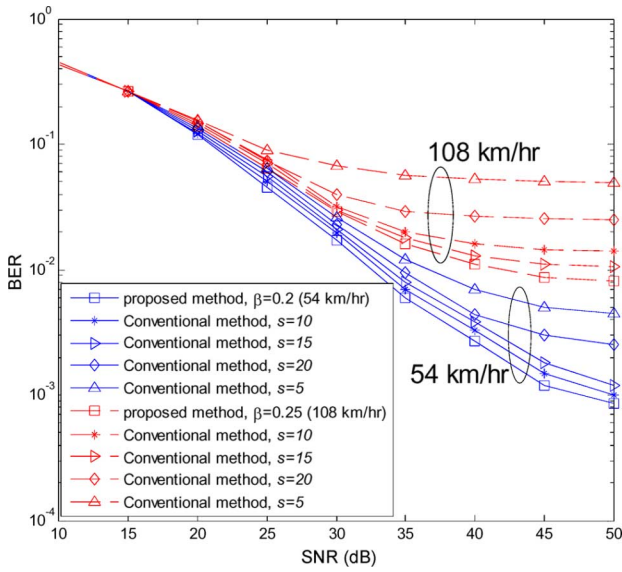


Fig. 15. Comparison of BER curves in the Jakes time-varying channel model for the proposed STO compensation method and the conventional approach with different forward-shift samples.

has larger estimation error than the methods using the CIR estimation approach [17]–[19] such that we need to advance the FFT position with a small forward-shift offset s for the conventional approach. In this simulation, the conventional method determines the start position of the FFT window by

$$\theta_{FFT} = -\theta_{coarse} + s_{pre-advance} - \theta_{residual} + s$$

where the value of θ_{FFT} is controlled to be a positive number, i.e. $\theta_{FFT} \geq 0$, according to the sign definition in (2). The coarse STO estimation θ_{coarse} gives the rough estimation first. To prevent ISI caused by the coarse STO estimation error, the first forward-shift $s_{pre-advance}$ is then added. The residual STO position $\theta_{residual}$ is estimated by (25) to obtain the fine STO position. The small offset s (usually a few samples) is used to prevent the possibility of the residual STO estimation error inducing ISI. This fine STO estimation error with a few samples of variation was also observed even by the complicated CIR approach [18], [23]. In Fig. 13, we can find that the best offset is about $s = 10$. For s being larger than 10, for example $s = 15$ or $s = 20$, the performance becomes worse. If the offset is not enough, ISI causes significant performance degradation even when $s = 7$. However, the best offset value s chosen for the case in Fig. 13 is not necessarily the best one for the case in Fig. 14. Similar simulation results for the Jakes time-varying case of the first 8 multipath taps used in the previous multipath Rayleigh fading channel with mobile speeds 54 km/hr and 108 km/hr are shown in Fig. 15, where we slightly increase the value of β for better parameter tracking capability in the time-varying environment. Thus, we can see that the best window offset value for the fine STO estimate is usually unknown in practice by using conventional approaches. The proposed method does not require the offset value s , thus its performance approaches the best case applying the conventional method.

V. CONCLUSION

In the conventional STO estimation process, the coarse STO estimation is used to find the proper FFT window position to prevent ISI. The fine STO estimation provides the better STO estimate to relieve the STO effect. From our study, a residual STO can cause significant performance degradation, especially with channel estimation obtained by interpolating the channel responses at pilot subcarriers. However, lots of pilots are usually needed to obtain an accurate STO estimate and hence intensive computations will be involved. In this paper, we analyze the effect of a positive STO value on the equalized output for an OFDM system applying linear channel interpolation. A new STO compensation technique is proposed for channel correction without concerning the estimation error possibly causing ISI due to the fine STO estimation algorithm, thus a simple residual STO estimation method can be used with less number of pilots compared to conventional approaches. In addition, the new method has the advantage of performance because no forward-shift sample is required for the FFT window. In contrast, the conventional methods usually require more than 10 forward-shift samples in our simulation cases and the performance is thus degraded due to the interpolation of the channel responses with rotated phases.

REFERENCES

- [1] "Digital Video Broadcasting (DVB): Framing structure, channel coding and modulation for digital terrestrial television," Draft EN 300 744 v1.4.1 (2001-01).
- [2] P. H. Moose, "A technique for orthogonal frequency division multiplexing frequency offset correcting," *IEEE Trans. Commun.*, vol. 42, no. 10, pp. 2908–2914, Oct. 1994.
- [3] E. S. Shim, S. T. Kim, H. K. Song, and Y. H. You, "OFDM carrier frequency offset estimation methods with improved performance," *IEEE Trans. Broadcast.*, vol. 53, no. 2, pp. 567–573, June 2007.
- [4] T. M. Schmidl and D. C. Cox, "Robust frequency and timing synchronization for OFDM," *IEEE Trans. Commun.*, vol. 45, no. 12, pp. 1613–1621, Dec. 1997.
- [5] M. Sliskovic, "Sampling frequency offset estimation and correction in OFDM systems," in *The 8th IEEE International Conference on Electronics, Circuits, and Systems (ICECS)*, Sep. 2001, vol. 1, pp. 437–440.
- [6] G. Ren, Y. Chang, H. Zhang, and H. Zhang, "Synchronization method based on a new constant envelop preamble for OFDM systems," *IEEE Trans. Broadcast.*, vol. 51, no. 1, pp. 139–143, Mar. 2005.
- [7] J. J. van de Beek, M. Sandell, and P. O. Borjesson, "ML estimation of time and frequency offset in OFDM systems," *IEEE Trans. Signal Processing*, vol. 45, no. 7, pp. 1800–1805, July 1997.
- [8] C. P. Li and W. W. Hu, "Super-imposed training scheme for timing and frequency synchronization in OFDM systems," *IEEE Trans. Broadcast.*, vol. 53, no. 2, pp. 574–583, June 2007.
- [9] M. Zao, A. Huang, Z. Zhang, and P. Qiu, "All digital tracking loop for OFDM symbol timing," in *2003 IEEE 58th Vehicular Technology Conference*, Oct. 2003, vol. 4, pp. 2435–2439.
- [10] S. H. Chen, W. H. He, H. S. Chen, and Y. Lee, "Mode detection, synchronization, and channel estimation for DVB-T OFDM receiver," in *IEEE Global Telecommunications Conference*, Nov. 2003, vol. 5, pp. 2416–2420.
- [11] C. H. Huang, S. C. Chen, and D. C. Chang, "A study on joint effect of synchronization and channel estimation in the DVB-T receiver," in *2005 8th International Symposium on Communications (ISCCom 2005)*, Kaohsiung, Taiwan, Nov. 2005.
- [12] J. Park, J. Kim, C. Kang, and D. Hong, "Channel estimation performance analysis for comb-type pilot-aided OFDM systems with residual timing offset," in *IEEE 60th Vehicular Technology Conference (VTC2004-Fall)*, Sep. 2004, vol. 6, pp. 4376–4379.
- [13] C. C. Ko, R. Mo, and M. Shi, "A new data rotation based CP synchronization scheme for OFDM systems," *IEEE Trans. Broadcast.*, vol. 51, no. 3, pp. 315–321, Sep. 2005.

- [14] P. Liu *et al.*, "A novel symbol synchronization scheme for OFDM," in *2005 International Conference on Communications, Circuits and Systems*, May 2005, vol. 1, pp. 247–251.
- [15] A. I. Bo, G. E. Jiann-hua, and W. Yong, "Symbol synchronization technique in COFDM systems," *IEEE Trans. Broadcast.*, vol. 50, no. 1, pp. 56–62, Mar. 2004.
- [16] Y. J. Ryu and D. S. Han, "Timing phase estimator overcoming Rayleigh fading for OFDM systems," *IEEE Trans. Consumer Electron.*, vol. 47, no. 3, pp. 370–376, Aug. 2001.
- [17] M. Speth, S. Fechtel, G. Fock, and H. Meyr, "Optimum receiver design for OFDM-based broadband transmission-Part II: A case study," *IEEE Trans. Commun.*, vol. 49, no. 4, pp. 571–578, Apr. 2001.
- [18] B. Yang, K. B. Letaief, R. S. Cheng, and Z. Cao, "Timing recovery for OFDM transmission," *IEEE J. Select. Areas Commun.*, vol. 18, no. 11, pp. 2278–2291, Nov. 2000.
- [19] A. Palin and J. Rinne, "Symbol synchronization in OFDM system for time selective channel conditions," in *The 6th IEEE International Conference on Electronics, Circuits and Systems*, Sep. 1999, vol. 3, pp. 1581–1584.
- [20] D. K. Kim *et al.*, "A new joint algorithm of symbol timing recovery and sampling clock adjustment for OFDM systems," *IEEE Trans. Consumer Electron.*, vol. 44, no. 3, pp. 1142–1149, Aug. 1998.
- [21] D. Lee and K. Cheun, "A new symbol timing recovery algorithm for OFDM systems," *IEEE Trans. Consumer Electron.*, vol. 43, no. 3, pp. 767–774, June 1997.
- [22] B. Ai, Z. X. Yang, C. Y. Pan, J. H. Ge, Y. Wang, and Z. Lu, "On the synchronization techniques for wireless OFDM systems," *IEEE Trans. Broadcast.*, vol. 52, no. 2, pp. 236–244, June 2006.
- [23] C. H. Huang, "Design and Implementation of the DVB-T Synchronization System," Master Thesis, Department of Communication Engineering, National Central University, Taoyuang, Taiwan, July 2005.
- [24] Y. J. Chen, Y. C. Lei, and T. D. Chiueh, "Baseband transceiver design for the DVB-terrestrial standard," in *The 2004 IEEE Asia-Pacific Conference on Circuits and Systems*, Dec. 2004, pp. 389–392.
- [25] P. Hoeher, S. Kaiser, and P. Robertson, "Two-dimensional pilot-symbol-aided channel estimation by Wiener filtering," in *Proc. of IEEE International Conference Acoustics, Speech, and Signal Processing*, Apr. 1997, vol. 3, pp. 1845–1848.
- [26] M. Li and W. Zhang, "A novel method of carrier frequency offset estimation for OFDM systems," *IEEE Trans. Consumer Electron.*, vol. 49, no. 4, pp. 965–972, Nov. 2003.
- [27] L. Schwoerer, "Fast pilot synchronization schemes for DVB-H," in *Proc. of the 4th IASTED International Multi-Conference Wireless and Optical Communications*, July 2004, pp. 420–424.



Dah-Chung Chang received the B.S. degree in electronic engineering from Fu-Jen Catholic University, Taipei, in 1991 and M.S. and Ph.D. degrees in electrical engineering from National Chiao Tung University, Hsinchu, in 1993 and 1998, respectively. In 1998 he joined Computer and Communications Research Laboratories at Industrial Technology Research Institute, Hsinchu. Since 2003, he has been a faculty member in the department of communication engineering at National Central University. His recent research interests include multirate and adaptive digital

signal processing, OFDM, and digital transceiver algorithm and architecture design.